Live imaging of bacterial actin MreBs causing helicity switching of a minimal synthetic cell

Yoshiki Tanaka[1], Hana Kiyama[2], Yusuke V. Morimoto[3], Makoto Miyata[2]

[1]Dept. Phys., Gakushuin Univ., [2]Grad. Sch. Sci., Osaka Metropolitan Univ., [3]Fac. Comp. Sci. and Sys. Eng., Kyushu Inst. Tech.

Abstract

Spiroplasma swim by shifting their helical body into right-handed and left-handed. Bacterial actin, MreB4 and MreB5 are involved in this helicity formation and shifting. Fluorescent labeling of each MreB and manipulating expression levels revealed that MreB4 is more structurally constrained and lower expression level required for motility than MreB5. Photobleaching and photoactivation indicated that MreB5 remains in place during movement. Treatment with MreB polymerization inhibitor A22 caused helix deformation, movement stall, and diffusion of MreB5 fluorescence. This indicates that A22 disrupts MreB5 interactions that are required for movement. These results have several implications for the mechanism and suggest that frequent MreB5 replacement during cell movement is unlikely.

Introduction

Spiroplasma. eriocheiris is a wall-less bacterium belonging to the class Molicutes [1, 2] and is parasitic to plants and crustaceans [3]. It swims by shifting its helical handedness between right and left, pushing water backward by rotating the body after the kink produced by helicity shifting. This motility resembles that of spirochetes in that it rotates the helix, but has no structural similarities in the machineries [4-6]. A ribbon-like structure located along the innermost line of the helix is related to the motility [5, 7]. This structure is composed of the *Spiroplasma*-specific protein Fibril, and five actin homologs MreB1-5 [7-11]. Experiments using the minimal synthetic bacterium JCVI-syn3B have shown that helicity shifting can be reconstituted by specific MreB pairs, MreB5-4, 5-1, 2-4, and 2-1 [12]. JCVI-syn3B was created by the J. Craig Venter Institute (JCVI) that has a genome with a minimal set of genes for growth derived from *Mycoplasma mycoides* [13, 14]. These motions induced by the two MreB types may be potentially applicable as actuators to generate artificial movements in liposomes and other synthetic systems. MreB is a bacterial actin homolog typically act as a scaffold for cell wall synthesis and is not directly related to motility in most bacteria [15]. In contrast, eukaryotic actin drives motility by two mechanisms. One is myosin rails, and the other is filament elongation and shortening coupled with polymerization and depolymerization. Although bacterial actin such as ParM and MamK exhibit dynamic polymerization [16, 17], Spiroplasma motility seems to follow a distinct mechanism [3]. No myosin genes are found in non-eukaryotes [18], and no significant loss of MreB fibers has been observed during helix inversion. However, further analysis is needed to conclude this. MreB generally has polymerization ability and ATPase activity like eukaryotic actin [19]. In *Spiroplasma*, MreB5 polymerizes into filaments in the presence of ATP and Mg2+ and has ATPase activity [20]. MreB1, thought to function similarly as MreB4, has higher ATPase activity [21]. However, how MreB4 and MreB5 differ functionally and how they behave during the movement remains unknown. The present study investigates the functional difference of two MreBs and the

dynamics of fluorescently labeled MreB5 in the minimal synthetic bacterium. We aim to complement existing structural and biochemical data, in order to propose a comprehensive model in the future. Here, we tracked MreB5 labeled with mCherry immediately after Y218 out of the total 350 residues [12].

Results and Discussion

New constructs

To examine the roles of MreB5 in elongation and motility, we observed the localization of mCherry-labeled MreB5 (MreB5m) in various forms of cells. Since the previous transformants [12] had low MreB expression levels, we replaced the promoter to the native one existing upstream of MreB4 (PmreB4) in the S. eriocheiris genome. In the new strain, the expression of MreB4 and 5 was 2.6 ± 0.4- and 9.3 ± 1.1-fold higher than those in the previous strain, respectively. The ratio of moving cells increased from 17.5% to 50.4% (Fig. S1a, Movie. S1). Previous strains expressing only MreB4 or MreB5 under the Pspi promoter did not show helical shape or movements [12]. However, new strains under PmreB4 promoter resulted in some helical but immotile cells (Fig. S1b). The protein amounts estimated from band intensity were 43 ± 7 and 14 ± 3-fold higher than the previous strains for MreB4 and MreB5, respectively.

Localization of fluorescently labeled MreBs

A partial signal was found in almost all the cells, positioning at helical and moving parts (Fig. 1 left), indicating that MreB5 is essential for helix formation.

To examine the subcellular localization of MreB4, we labeled it by inserting mCherry immediately after Y225, a position corresponding to the labeling site of MreB5. Signals were observed in almost all the cells, and some cells showed helical morphology. However, no moving cells were observed (Fig. 1 right). Then, we shifted the insertion positions per one residue, however none of the 14 constructs tested showed movements (Movie. S2). We also tried to label MreB4 by Tetracysteine (TC) motif composed of only 12 residues. Biarsenical dye called FlAsH is expected to bind this motif and emit fluorescence [22, 23]. TC motif was fused at N-terminus, C-terminus, and immediately after Y225 of MreB4. The construct inserted immediately after Y225 showed 5 cells moving out of approximately 500 (Movie. S3-5). However, the kink propagation was not observed, and the background fluorescence due to FlAsH was high. We concluded that the TC labeling was not suitable because of the low motile cell ratio and fluorescence S/N ratio to follow MreB cellular dynamics. The difficulty in fluorescent labeling of MreB4 may suggest that MreB4 interacts with other structures through larger numbers of positions than MreB5.

Relation between quantity ratio of two MreBs and motility

We examined the quantity ratio of two MreBs at which movements were observed. We constructed a strain with a constitutive expressing MreB and another inducible one. In these strains, one MreB is under the control of the Pxyl/tetO2 promoter, where the expression is prevented by a tetracycline repressor (TetR) [24]. The MreB expression was induced by adding 9 μM tetracycline. The protein levels and ratio of motile cells were analyzed (Fig. 2ab). In the strain expressing both MreBs constitutively, the ratio of moving cell was 19 %. In the strain only MreB5m is constitutively expressed, inducing MreB4 to 20 % of the constitutive level resulted in 16 % motile cells. On the other hand, in the strain only MreB4 is expressed constitutively, inducing MreB5m to 25 % resulted in 3 % motile cells. Higher requirement of MreB5 than MreB4 to move the cells may suggest that MreB5 serves as the backbone of the helix and that MreB4 causes MreB5 helix inversion. It should be noted that the expression level

shown here is for the culture as a whole and not for within a single cell.

MreB5 replacement traced fluorescently by photobleaching and photoactivation

To examine whether frequent polymerization-depolymerization is involved in the motility, we focused on MreB5m behaviors in a motile cell. The FRAP (Fluorescence Recovery After Photobleaching) method is a technique to estimate the diffusion rate of target proteins from the recovery rate of the fluorescence intensity at the area photobleached by intense excitation light [25]. If frequent replacement of MreB5 subunit occurs, fluorescence should recover rapidly. Here, we focused on cells that were attached to the glass only at both poles and stretched by liquid flow applied before observation. These cells exhibited movement, although the kink propagation did not fully reached the pole due to the attachment. We bleached one end of such cell and traced the fluorescence intensities and showed a kymograph (Fig. 3a). In the strain expressing MreB4 and MreB5m (Fig. 3a upper), fluorescence intensity dropped to about 10 % of initial value and reached to a plateau at about 30% within 5 seconds. The recovery was not observed in chemically fixed cells (Fig. 3a bottom). In the strain expressing free mCherry additionally to MreB4 and MreB5 (Fig. 3a middle), the post-bleach intensity recovered to about 50% within 5 seconds. The latter two results indicate that the value does not recover for not fluid protein such as chemically fixed MreB5m. It recovers quickly for highly fluid proteins such as non-fused mCherry. In the strain expressing MreB4 and MreB5-mCherry, the recovery to 30% indicates the presence of highly fluid MreB5m. However, the lack of subsequent recovery suggests that the remaining MreB5m stayed. As another tracking method, we used PAmCherry (Photoacitivatable mCherry) [26]. This protein is initially non-fluorescent and activated by UV irradiation. This is caused by only 10 amino acid modification from mCherry. MreB5 fused with PAmCherry worked as mCherry. Then, we irradiated the cells with UV light, and traced the subsequent brightness (Fig. 3b). After UV irradiation, only the irradiated area exhibited fluorescence in both over 12 seconds and 8 min timescale. These results indicate that MreB5 remains in the same cellular position during movements, without obvious replacements.

Effect of MreB Polymerization Inhibitor A22 on cell movements and MreB5 Localization

To examine the role of the polymerization ability of MreB, we added the MreB polymerization inhibitor A22. A22 is a small compound with a molecular weight of 271.6 and has been shown to bind the nucleotide binding site of *Caulobacter Crescentus* MreB [27, 28]. However, it remains unclear whether A22 also binds to *Spiroplasma* MreB and inhibits polymerization. Addition of 250 μM of A22 to the cell expressing MreB4 and MreB5m linearized the helix, and stalled movements over 150 seconds (Fig. 4a). In the FRAP observation, fluorescence that once reached a plateau recovered by 20 % after A22 addition (n=2) (Fig. 4b). In the cell expressing MreB4 and MreB5-PAmCherry, fluorescence of the specific photoactivated region has spread 100 seconds after A22 addition (Fig. 4c). These results indicate that A22 inhibited some interaction responsible for keeping MreB5 molecules in the same cellular position. On the other hand, FRAP observation for the cells linearized by A22, showed no fluorescence recovery (Fig. 4d). Therefore, A22 may inhibit certain interaction of MreB5 but does not increase the fluidity. MreB5m may aggregate by other interaction than which inhibited by A22. This is also supported by the uneven fluorescence distribution after A22 addition. A22 removal caused helix reformation immediately and the motility recovered within 10 seconds (Fig. 4a), with various speed. Both helix linearization and reformation occurred along the entire cell length, MreB5 unlikely detach from the ends. Cells with labeled MreB4 or without MreB4 forms non-motile helix, which did not linearized by A22. In one of the exceptions, approximately 40% was linearized after 110 till 175 seconds from A22 addition (Fig. 4a). This suggests that the A22 binding site of MreB5 is not accessible in the absence of cell movements. During movements, A22 possibly become able to affect MreB5 either by a conformational change in MreB5 or destabilization of the internal structure.

Conclusion

This study suggests (i) Two MreBs have distinct functions, (ii) MreB5 does not have a dynamic replacement unlike a treadmilling of eukaryotic actin. Then, the remaining questions are how the polymerization ability and ATPase activity of MreB5 are related to this, how structural change without dynamic replacements affect the orientation of the helix, why interactions with A22 occur at that time. In addition to examining the dynamics of MreB4, further studies are required.

Materials and Methods

Bacterial strains and culture conditions

S. eriocheiris (TDA-040725-5T) and JCVI-syn3B (GenBank, CP069345.1) were cultured in SP4 medium [29] at 30℃ and 37℃, respectively, until they reached an optical density of 0.02–0.03 at620 nm. For DNA manipulation, *Escherichia coli* strains DH5α and iVEC3 were used.

Gene manipulation of syn3B

DNA manipulation and JCVI-syn3B transformation were performed as previously described ([30-32]). Plasmids and primers used in this study are listed in Figure S3 and Table S1, respectively. pSeN540 and pSeN540mC5 were prepared from pSeW545 and pSeW545-F5 (1), respectively by replacing the Ptuf promoter with the native promoter of MreB4. The tetracycline-inducible module was introduced from pSD079. A codon optimized PAmCherry gene was synthesized by the GenTitan Gene Fragment service (Genscript, Tokyo, Japan).

Cell treatments and optical microscopy

The following methods were used unless otherwise described. The cultured cells were centrifuged at 8,000 × g for 5 min and suspended with supernatant at 5−fold cell density if the cell density is not enough. The cell suspension was mixed in a ratio of 3:2 with a solution consisting of 20 mM HEPES, 330 mM NaCl, 0.8% methylcellulose, and flowed into the tunnel chamber [33] made with coverslips cleaned by KOH saturated ethanol. After 5−10 minutes set for cell adhesion, the liquid was replaced with 30 µl of a solution consisting of 0.4% Methylcellulose, 20 mM HEPES, 330 mM NaCl to remove non-adherent cells. In the case of A22 treatment, 10 mM A22 (Cayman Chemical Company, Michigan, America) stock solution was dissolved in DMSO. The liquid in a tunnel was replaced with a solution consisting of 250 µM A22, 20 mM HEPES, 330 mM NaCl, 0.4% Methylcellulose for A22 addition. Cells were observed by an Evident inverted microscope IX71 with a UPlanSApo 100×/1.4 NA Ph3 and CMOS camera (DMK33UX174, The Imaging Source, Bremen, Germany). Images were captured at 30FPS. Images were analyzed by ImageJ 1.54g.

About protein profile

For the expression induction, Tetracycline dissolved in ethanol at 4 mg/ml was added to the culture at a final concentration of 0.4 μg/ml. The culture was then incubated at 37℃ for various times, subjected to the SDS-10% PAGE. Loading volumes were normalized by culture ODs. For the identification of moving parts, the minimum intensity projection (Image > Stack > Z projection) was subtracted from each frame. For the comparison of promoter, each sample was subjected to the SDS-12.5 % PAGE. The cultured cells were centrifuged at 9,000 × g for 8 min and suspended with a solution consisting of 1 × PBS, 20mM Sucrose at 20-fold cell density for observation.

FRAP

Cells were observed by an Evident inverted microscope IX83 with a UPlanSApo 100× /1.45 NA Ph3 and EMCCD camera (ixon897, Andor, Belfast, UK). Images were captured at 40FPS. Fluorescence imaging was done with 10% of the maximum intensity of LED light source (Evident U-LGPS) and manually switched to the maximum intensity with the minimum aperture during bleaching. Timelapse was captured at 1FPS. For chemical fixation, 4-5m strain was mixed in a ratio of 1:1 with a 0.8% paraformaldehyde solution, incubated at 22 − 27 ℃ for 10 min, rinsed with 1M glycine. Fixed cells were centrifuged at 12,000 × g for 10 min at 10 °C and suspended with a solution consising of 20 mM HEPES, 330 mM NaCl at 2-fold density of the culture. Due to the small size of JCVI-syn3B, it was not possible to create a circular bleached area, as is typically done in FRAP. Additionally, tracking fluorescence intensity at a specific region was challenging due to cell movement. Therefore, the edges of cells that adhered linearly to the glass surface were bleached, and pixel values were profiled along a five-pixel-wide vertical band along the cell axis. The fluorescence intensity of a frame was quantified by subtracting the minimum value from the maximum value in the selected regions.

Photoactivation

For UV irradiation at the precise part of the cell, a pattern illuminator (LEOPARD2-White, OPTO-LINE Saitama, Japan) was used. In this setup, cells were observed by IX73 equipped with an sCMOS camera (Zyla4.2, Andor, UK). The filters used to detect mCherry and PAmCherry were Evident IX3-FMCHEXL (Ex.565-585 nm, Dichroic.595 nm, Em.600-690).The wavelength of UV used for photoactivation of PAmCherry distributed 352-402 nm.

Reference

1. Kakizawa, S. and M. Mizutani, *Overview of the new Genus names for Mycoplasmas.* Japanese Society of Microbial Ecology, 2025. **40**(1): p. 29-37.
2. Wang, Y., et al., *Phylogenomics of expanding uncultured environmental Tenericutes*

provides insights into their pathogenicity and evolutionary relationship with Bacilli. BMC Genomics, 2020. **21**(1): p. 408.

3. Harne, S., P. Gayathri, and L. Beven, *Exploring Spiroplasma Biology: Opportunities and Challenges.* Front Microbiol, 2020. **11**: p. 589279.
4. Shaevitz, J.W., J.Y. Lee, and D.A. Fletcher, *Spiroplasma swim by a processive change in body helicity.* Cell, 2005. **122**(6): p. 941-5.
5. Kurner, J., A.S. Frangakis, and W. Baumeister, *Cryo-electron tomography reveals the cytoskeletal structure of Spiroplasma melliferum.* Science, 2005. **307**(5708): p. 436-8.
6. Nakane, D., T. Ito, and T. Nishizaka, *Coexistence of Two Chiral Helices Produces Kink Translation in Spiroplasma Swimming.* J Bacteriol, 2020. **202**(8).
7. Liu, P., et al., *Chemotaxis without Conventional Two-Component System, Based on Cell Polarity and Aerobic Conditions in Helicity-Switching Swimming of Spiroplasma eriocheiris.* Front Microbiol, 2017. **8**: p. 58.
8. Sasajima, Y., et al., *Isolation and structure of the fibril protein, a major component of the internal ribbon for Spiroplasma swimming.* Front Microbiol, 2022. **13**: p. 1004601.
9. Trachtenberg, S., et al., *Structure of the cytoskeleton of Spiroplasma melliferum BC3 and its interactions with the cell membrane.* J Mol Biol, 2008. **378**(4): p. 778-89.
10. Williamson, D.L., J. Renaudin, and J.M. Bove, *Nucleotide sequence of the Spiroplasma citri fibril protein gene.* J Bacteriol, 1991. **173**(14): p. 4353-62.
11. Ku, C., W.S. Lo, and C.H. Kuo, *Molecular evolution of the actin-like MreB protein gene family in wall-less bacteria.* Biochem Biophys Res Commun, 2014. **446**(4): p. 927-32.
12. Kiyama, H., et al., *Reconstitution of a minimal motility system based on Spiroplasma swimming by two bacterial actins in a synthetic minimal bacterium.* Sci Adv, 2022. **8**(48): p. eabo7490.
13. Hutchison, C.A., 3rd, et al., *Design and synthesis of a minimal bacterial genome.* Science, 2016. **351**(6280): p. aad6253.
14. Pelletier, J.F., et al., *Genetic requirements for cell division in a genomically minimal cell.* Cell, 2021. **184**(9): p. 2430-2440 e16.
15. Shi, H., et al., *How to Build a Bacterial Cell: MreB as the Foreman of E. coli Construction.* Cell, 2018. **172**(6): p. 1294-1305.
16. Popp, D. and R.C. Robinson, *Many ways to build an actin filament.* Mol Microbiol, 2011. **80**(2): p. 300-8.
17. Charles-Orszag, A., N.A. Petek-Seoane, and R.D. Mullins, *Archaeal actins and the origin of a multi-functional cytoskeleton.* J Bacteriol, 2024. **206**(3): p. e0034823.
18. Miyata, M., et al., *Tree of motility - A proposed history of motility systems in the tree of life.* Genes Cells, 2020. **25**(1): p. 6-21.

19. van den Ent, F., L.A. Amos, and J. Lowe, *Prokaryotic origin of the actin cytoskeleton.* Nature, 2001. **413**(6851): p. 39-44.
20. Takahashi, D., I. Fujiwara, and M. Miyata, *Purification and ATPase Activity Measurement of Spiroplasma MreB.* Methods Mol Biol, 2023. **2646**: p. 359-371.
21. Takahashi, D., et al., *A highly active bacterial actin actuates the polymerization of another isoform essential for swimming motility of Spiroplasma.* bioRxiv, 2025: p. 2024.09.04.611326.
22. Griffin, B.A., S.R. Adams, and R.Y. Tsien, *Specific covalent labeling of recombinant protein molecules inside live cells.* Science, 1998. **281**(5374): p. 269-72.
23. Martin, B.R., et al., *Mammalian cell-based optimization of the biarsenical-binding tetracysteine motif for improved fluorescence and affinity.* Nat Biotechnol, 2005. **23**(10): p. 1308-14.
24. Mariscal, A.M., et al., *Tuning Gene Activity by Inducible and Targeted Regulation of Gene Expression in Minimal Bacterial Cells.* ACS Synth Biol, 2018. **7**(6): p. 1538-1552.
25. Esue, O., et al., *Dynamics of the bacterial intermediate filament crescentin in vitro and in vivo.* PLoS One, 2010. **5**(1): p. e8855.
26. Subach, F.V., et al., *Photoactivatable mCherry for high-resolution two-color fluorescence microscopy.* Nat Methods, 2009. **6**(2): p. 153-9.
27. Iwai, N., K. Nagai, and M. Wachi, *Novel S-benzylisothiourea compound that induces spherical cells in Escherichia coli probably by acting on a rod-shape-determining protein(s) other than penicillin-binding protein 2.* Biosci Biotechnol Biochem, 2002. **66**(12): p. 2658-62.
28. van den Ent, F., et al., *Bacterial actin MreB forms antiparallel double filaments.* Elife, 2014. **3**: p. e02634.
29. Tully, J.G., et al., *Enhanced isolation of Mycoplasma pneumoniae from throat washings with a newly-modified culture medium.* J Infect Dis, 1979. **139**(4): p. 478-82.
30. Karas, B.J., et al., *Rescue of mutant fitness defects using in vitro reconstituted designer transposons in Mycoplasma mycoides.* Front Microbiol, 2014. **5**: p. 369.
31. Mizutani, M., et al., *Robust and highly efficient transformation method for a minimal mycoplasma cell.* J Bacteriol, 2025. **207**(3): p. e0041524.
32. Uenoyama, A., et al., *Rapid in vitro method to assemble and transfer DNA fragments into the JCVI-syn3B minimal synthetic bacterial genome through Cre/loxP system.* Biophys Physicobiol, 2024. **21**(4): p. e210024.
33. Kasai, T., T. Hamaguchi, and M. Miyata, *Gliding Motility of Mycoplasma mobile on Uniform Oligosaccharides.* J Bacteriol, 2015. **197**(18): p. 2952-7.

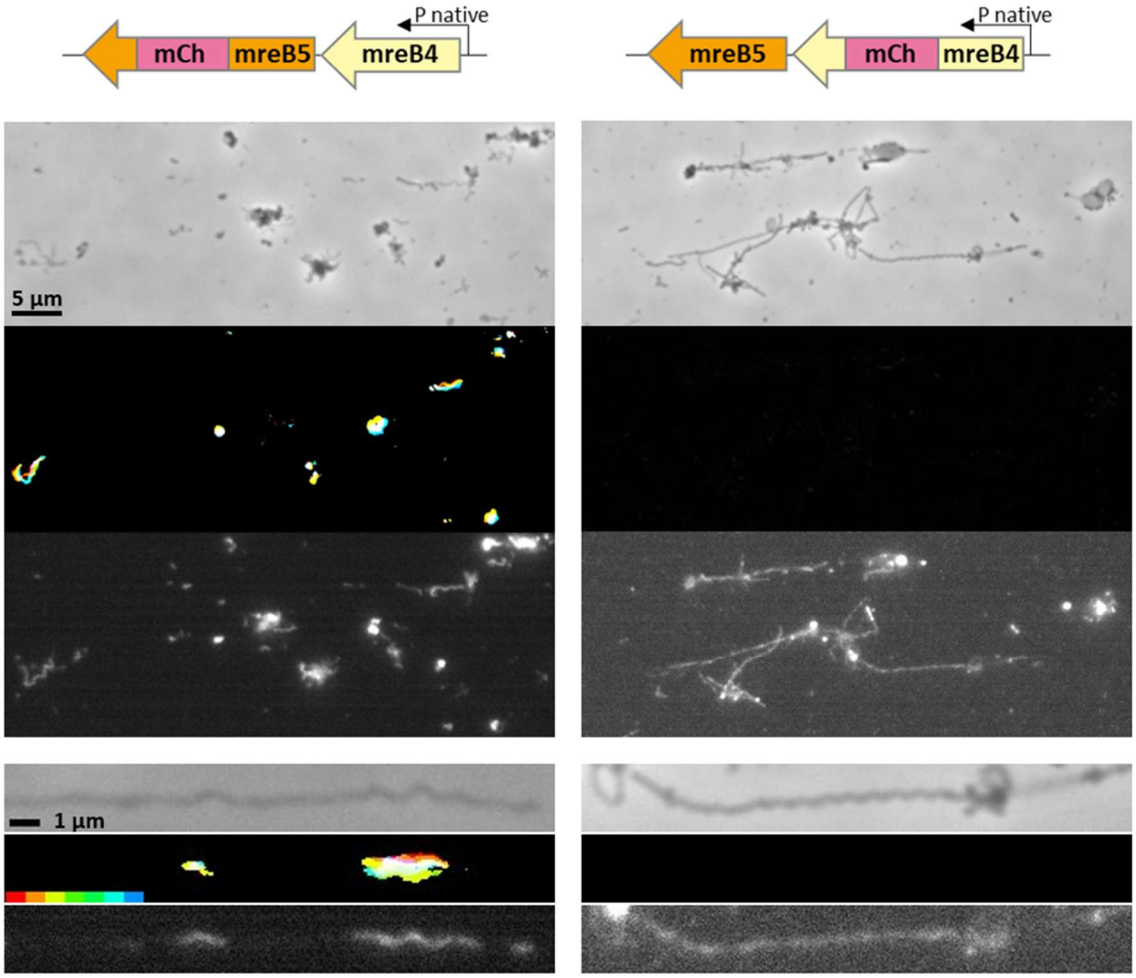

Fig. 1 Localization of each MreB labeled with mCherry. Gene constructs are illustrated at the top. Field and cell images are shown for phase contrast, rainbow-trace of moving part, fluorescence, from the top. Moving parts were colored red to blue shifting for total 7 frames. Excitation light 10- times brighter than MreB5-mCherry was irradiated for MreB4–mCherry.

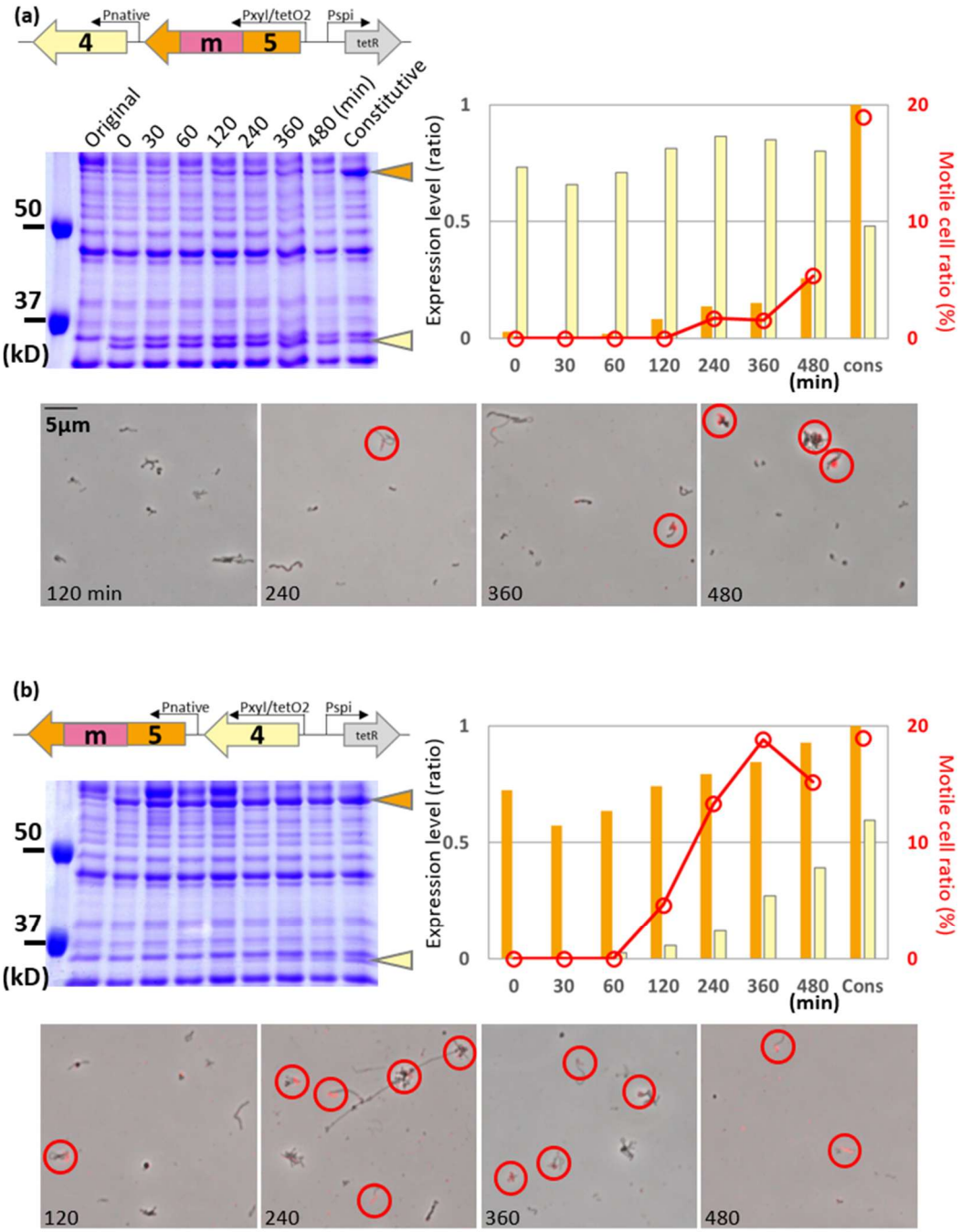

Fig. 2 Motile cell ratio at various times after one MreB induction in a background of constitutive expression of another MreB. (a) MreB5 induction to constitutive MreB4 expression. (b) MreB4 induction to constitutive MreB5 expression. Gene constructs are illustrated in upper left. Protein expression has induced and protein profiles at various induction times were analysed by SDS-10%-PAGE. The bands for MreB4 and MreB5m are shown by yellow and orange triangles respectively. Cell images at various induction times are indicated on the bottom. The parts that changed position over time were judged by substracting different frames and colored red. Motile cells are indicated by red circles. Upper right shows integrated result. Yellow and orange bars show the band intensity of MreB4 and MreB5m divided by molecular weight. Number on the left is normalized by MreB5m of strain pSeN540mc5. Red circles and number on the right show the ratio of motile cells.

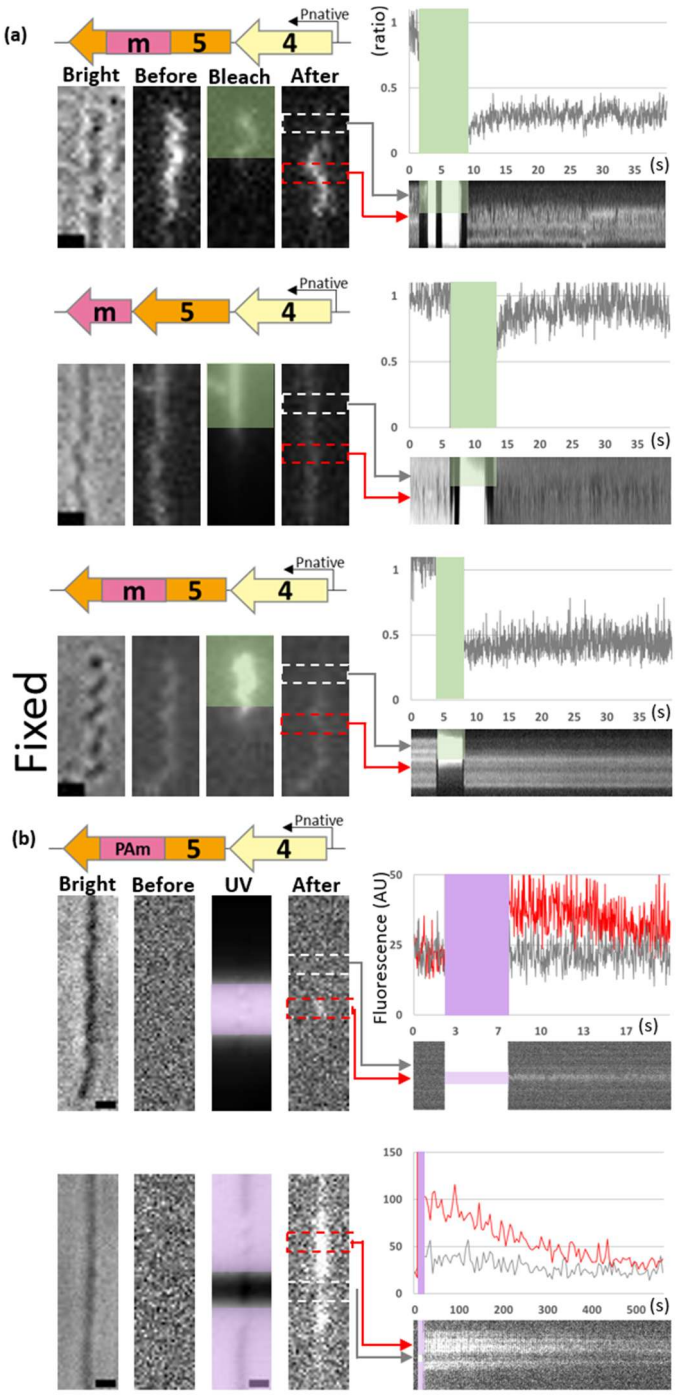

Fig. 3 MreB5 dynamics examined by photobleaching and photoactivation. Gene constructs are illustrated in the upper left. Cell images are shown on the left. Scale bar, 1μm. Fluorescence intensity is traced on the right. Kymographs are shown below each graph. **(a)** Photobleaching. Cell images in brightfield, prebleach, bleach, postbleach are shown from the left. Bleached area is shown by a green translucent square. Recovery of bleached fluorescence was traced for 40 s by measuring the fluorescence intensity ratio of white dotted area to red dotted area. Bleaching time is shown by a green rectangle. **(b)** Photoactivation. Cell images in brightfield, preactivation, UV irradiation, postactivation are shown from the left. UV irradiated area is shown by a purple translucent square. Fluorescence intensity for red and white dotted areas were traced. UV irradiation time is shown by a purple rectangle.

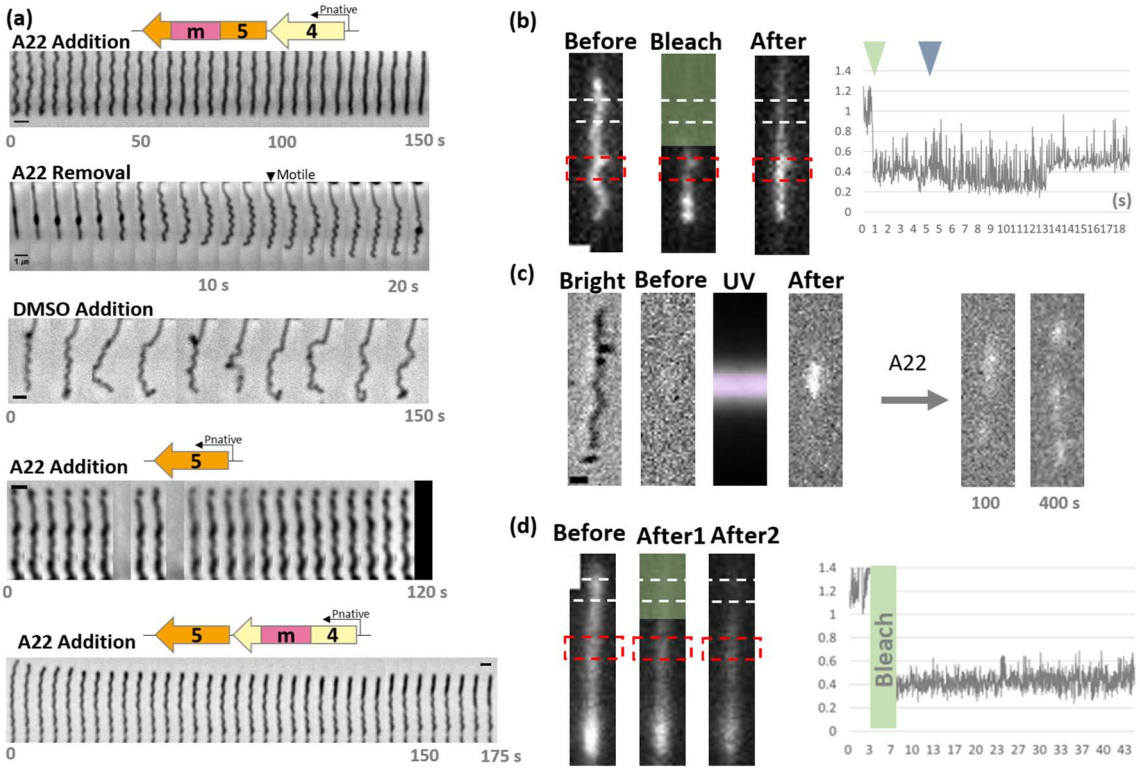

Fig. 4 Effect of A22 to cell motility, morphology, and MreB5m behavior. **(a)** Morphological change of cell after addition of A22 or DMSO and removal of A22. Gene constructs are illustrated above. **(b)** Effect of A22 on MreB5 dynamics examined by FRAP. A22 was added after bleaching. Cell images are shown for prebleach, bleach, postbleach from the left. Fluorescence intensity trace is shown on the right. Photobleaching and A22 addition were applied at a green and blue triangles respectively. **(c)** Effect of A22 on MreB5 dynamics examined by photoactivation. Cell images are shown for brightfield, preactivation, UV irradiation, postactivation, and 100, 400 s after A22 addition from the left. **(d)** Effect of A22 on MreB5 dynamics examined by FRAP. A22 was added before bleaching. Cell images are shown for prebleach, postbleach1, postbleach2 from the left. Fluorescence intensity trace is shown on the right.

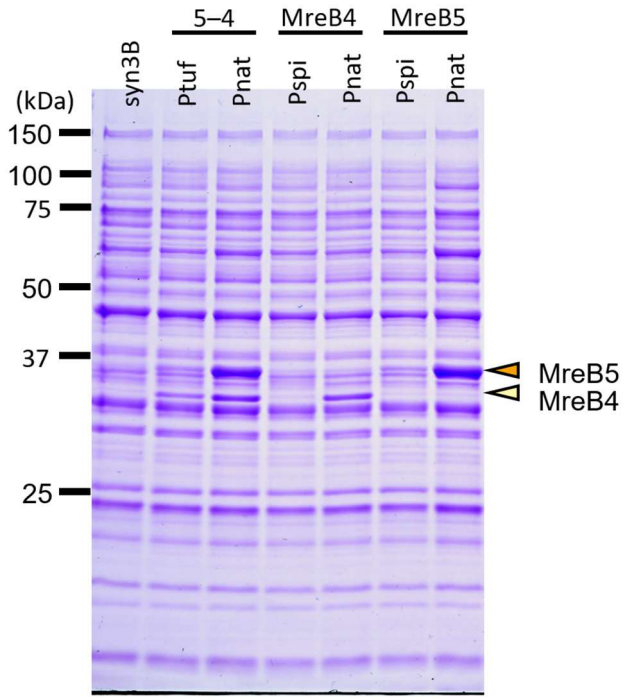

Fig. S1 Comparison of expression level of MreB4 and MreB5 between previous and improved promoters by SDS-12.5 % PAGE. The loaded sample was syn3B original, syn3B with MreB4 and MreB5, with MreB4, with MreB5 from the left. The bands for MreB4 and MreB5 are shown by yellow and orange triangles respectively.

(a)

Position	FP, Tag	Helix	Motility
N-ter	EYFP	×	×
	TC	○	×
K46-E47	EYFP	○	×
	TC	○	×
E218-I219	mCherry	○	×
I219-G220	mCherry	○	×
G220-S221	mCherry	△	×
S221-L222	mCherry	○	×
L222-A223	mCherry	○	×
A223-K224	mCherry	×	×
K224-Y225	mCherry	△	×
Y225-P226	mCherry	○	×
	TC	○	△
P226-D227	mCherry	○	×
D227-E228	mCherry	○	×
E228-R229	mCherry	○	×
R229-K230	mCherry	○	×
K230-M231	mCherry	○	×
C-ter	EYFP	○	×
	TC	△	×

(b)

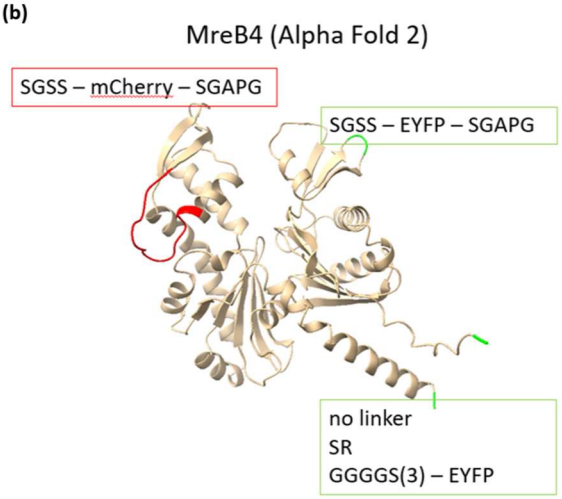

(c)

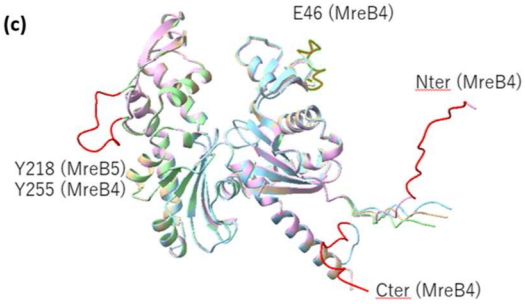

Fig. S2 Characteristic of transformants of MreB4 labeled with mCherry, EYFP, TC-tag. (a) The list for morphology and motility of various transformants. (b) Labeled positions indicated in predicted structure of MreB4. (c) Predicted structure of MreB4 labeled with TC-Tag.

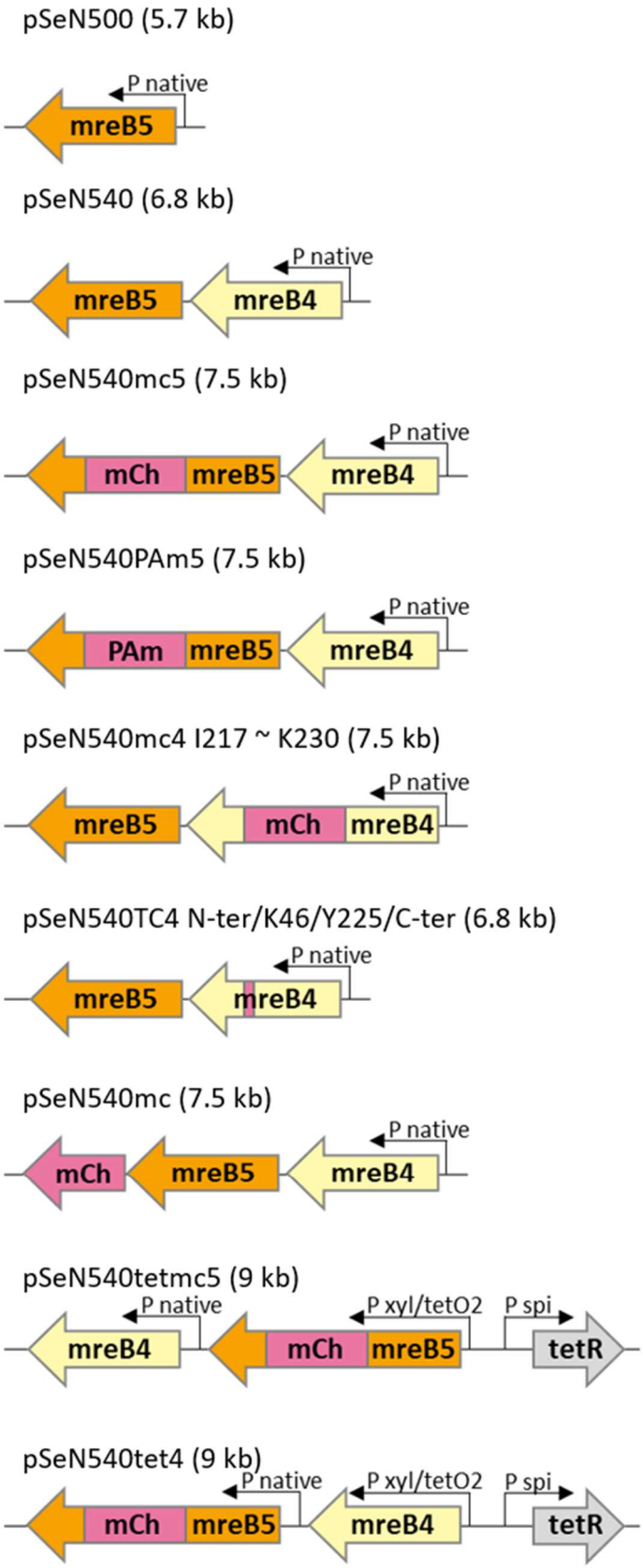

Fig.S3 Schematic presentation for DNA constructs used in this study.

Table. S1 DNA primers used in this study. Each of the word in rightmost column means, In: In-Fusion® HD Cloning Kit (Takara Bio Inc. Kusatsu, Japan), NEB: NEBuilder® HiFi DNA Assembly Master Mix (New England Biolabs, Inc., MA, USA) (19), iVEC3: fragments were assembled in Escherichia coli (iVEC3).

Name	Sequence	Purpose	Template	Assembly
Lp_inverse_F	AGGACTGAGCTAGCTGTCAAAGATC	pSeN540	pSD079	iVEC3
LP-inverse-R	GAACTATATAAATAACTCGCATATTG	pSeN540	pSD079	iVEC3
		pSeN400	pSeN540	iVEC3
		4-tet5m, 4-tet5	pSD079	In
opr-mreB4-5-079-F	AATATGCGAGTTATTTATATAGTTCATTTGGCATCCAAGAATAACG	pSeN540	*S. eriocheiris* genome	iVEC3
opr-mreB4-5-079-R	GATCTTTGACAGCTAGCTCAGTCCTCTATTGCTAATTTCAAGAAGTCAT	pSeN540	*S. eriocheiris* genome	iVEC3
N540_delMreB4_F	AAATATATTCTGTAAAAATTCCTCCCTTT	pSeN500	pSeN540	iVEC3
N540_delMreB4_R	AATTTTTACAGAATATATTTAGAGAAATTCGCTT	pSeN500	pSeN540	iVEC3
MreB4-F	GCGAGTTATTTATATAGTTCTTAGTAATCTAATTCTTTAGTATG	pSeN400	pSeN540	iVEC3
mreB5-mChe-link-F	ATAATAGCTGATGATCCTGAGTATTTAACTAATGAACCGATGTA	pSeN540mc5	pSeN540	In
mreB5-mChe-link-R	ATAAAAGTGGAGCTCCTGGTCATAATGAACGTGCAATGCAAATT	pSeN540mc5	pSeN540	In
SWmChe-linker-F	ACCAGGAGCTCCACTTTTATATAGTTCATCCATACCAC	pSeN540mc5	pSeW545-F5	In
SWmChe_linker_R2	TCAGGATCATCAGCTATTATTAAAGAATTT	pSeN540mc5	pSeW545-F5	In
del-dCas9-F	CTTGTTGCCTCCTTAGCAGATGCT	4-tet5m, 4-tet5	pSD079	In
Vector_MreB4_TY_F	GCGAGTTATTTATATAGTTCTTAGTAATCTAATTCTTTAGTATGC	4-tet5m, 4-tet5	pSeN540	In
MreB4_MreB5_TY_R	GATGCCAAATCTATTGCTAATTTCAAGAAGTCATT	4-tet5m, 4-tet5	pSeN540mc5	In
MreB4_MreB5_TY_F	TTAGCAATAGATTTGGCATCCAAGAATAACGGATT	4-tet5m, 4-tet5	pSeN540mc5	In
MreB5_vector_TY_R	TCTGCTAAGGAGGCAACAAGGTGAAACCAGAAAGACCATTTATCT	4-tet5m, 4-tet5	pSeN540	In
N540_delMreB4_F	AAATATATTCTGTAAAAATTCCTCCCTTT	5-tet4	4tet5m	NEB
TetMreB4_VR	AGATTACTAAGCTGGCATTGGGAAGAAA	5-tet4	4tet5m	NEB
TetMreB4_IF	CAATGCCAGCTTAGTAATCTAATTCTTTAGTATGCATTTGTTC	5-tet4	pSeN540	NEB
TetMreB4_IR	TCTGCTAAGGAGGCAACAAGATGGCAGGATTTAATAGC	5-tet4	pSeN540	NEB
del-dCas9-F	CTTGTTGCCTCCTTAGCAGATGCT	5-tet4	45tet5H	NEB
N540_delMreB4_R	AATTTTTACAGAATATATTTAGAGAAATTCGCTT	5-tet4	45tet5H	NEB
m_PAm_IF	TATCTAATTTTCTATTAACATTATAAGC	4-5PAmCherry	PAm-fragment	NEB
m_PAm_IR	TAATGGACATGTTTTTGAAATAGAAGGTG	4-5PAmCherry	PAm-fragment	NEB
PAm_m_VF	TTTCAAAAACATGTCCATTAACTGATCC	4-5PAmCherry	pSeN540mc5	NEB
PAm_m_VR	TGTTAATAGAAAATTAGATATTACTTCAC	4-5PAmCherry	pSeN540mc5	NEB
MreB5ter-mCherry-IF	TCTTGTTAATTATTTATATAGTTCATCCATACCAC	4-5-mCherry	pSeN540mc5	In
MreB5-MreB5SD-mCherry-IR	TATTAAGGAGGAAATTAACATGGCTATTATTAAAGAATT	4-5-mCherry	pSeN540mc5	In
mCherry-MreB5SD-MreB5-VF	TGTTAATTTCCTCCTTAATATTTATTTTTTCTTCCCAATG	4-5-mCherry	pSeN540	In
mCherry-MreB5ter-VR	GGATGAACTATATAAATAATTAACAAGATAAATTAAA	4-5-mCherry	pSeN540	In
syn3B-junc-F	TATGTGATAATGCCAATCGCTAAG	colonyPCR		
syn3B-junc-R	GTAAATTCCCAAATTATTCCATCA	colonyPCR		
MreB4_TC_Nter_F	TACAACAACCTGGACAACAATTTAAAAACATTGTAAAAATTCCTCC	4TC(Nter)-5	pSeN540	iVEC3
MreB4_TC_Nter_R	TTGTTGTCCAGGTTGTTGTATGGAACCAGCAGGATTTAATAGCGGC	4TC(Nter)-5	pSeN540	iVEC3
MreB4_TC_Cter_F	TACAACAACCTGGACAACAATTTAAAAAGTAATCTAATTCTTTAG	4TC(Cter)-5	pSeN540	iVEC3
MreB4_TC_Cter_R	TTGTTGTCCAGGTTGTTGTATGGAACCATAAAAAAGAATATATTTAG	4TC(Cter)-5	pSeN540	iVEC3
MreB4_TC_Y225P226_F	CAACAACCTGGACAACAATTTAAAAAGTATTTTGCTAATGAACC	4TC(Y225)-5	pSeN540	iVEC3
MreB4_TC_Y225P226_R	AATTGTTGTCCAGGTTGTTGTATGGAACCAGACGAAAGAAAAATG	4TC(Y225)-5	pSeN540	iVEC3
MreB4_TC_46K47E_F	TACAACAACCTGGACAACAATTTAAAAATTTTATTCTGTAAGCTAC	4TC(K46)-5	pSeN540	iVEC3
MreB4_TC_46K47E_R	TTGTTGTCCAGGTTGTTGTATGGAACCAGAAAATAGAATTATTGC	4TC(K46)-5	pSeN540	iVEC3
MreB5_TC_Y218H219_F	TACAACAACCTGGACAACAATTTAAAAAGTATTTAACTAATGAACC	4-5TC(Y218)	pSeN540	iVEC3
MreB5_TC_Y218H219_R	TTGTTGTCCAGGTTGTTGTATGGAACCACATAATGAACGTGCAATG	4-5TC(Y218)	pSeN540	iVEC3
SWmChe_linker_F2	ACCAGGAGCTCCACTTTTATATAG	4m-5	pSeN540mc5	In
SWmChe_linker_R2	TCAGGATCATCAGCTATTATTAAAGAATTT	4m-5	pSeN540mc5	In
pSeW217_F	ATAATAGCTGATGATCCTGAAATTTTAATTTGTTCAGC	4m-5	pSeN540	In
pSeW217_R	ATAAAAGTGGAGCTCCTGGTGAAATTGGTTCATTAGCAAA	4m-5	pSeN540	In
pSeW218_F	ATAATAGCTGATGATCCTGATTCAATTTTAATTTGTTCAG	4m-5	pSeN540	In
pSeW218_R	ATAAAAGTGGAGCTCCTGGTATTGGTTCATTAGCAAAATA	4m-5	pSeN540	In
pSeW219_F	ATAATAGCTGATGATCCTGAAATTTCAATTTTAATTTGTTC	4m-5	pSeN540	In
pSeW219_R	ATAAAAGTGGAGCTCCTGGTGGTTCATTAGCAAAATAC	4m-5	pSeN540	In
pSeW220_F	ATAATAGCTGATGATCCTGAACCAATTTCAATTTTAATTTG	4m-5	pSeN540	In
pSeW220_R	ATAAAAGTGGAGCTCCTGGTTCATTAGCAAAATACCCAG	4m-5	pSeN540	In
pSeW221_F	ATAATAGCTGATGATCCTGATGAACCAATTTCAATTTTAATTTG	4m-5	pSeN540	In
pSeW221_R	ATAAAAGTGGAGCTCCTGGTTTAGCAAAATACCCAGAC	4m-5	pSeN540	In
pSeW222_F	ATAATAGCTGATGATCCTGATAATGAACCAATTTCAATTTTAATTTG	4m-5	pSeN540	In
pSeW222_R	ATAAAAGTGGAGCTCCTGGTGCAAAATACCCAGACGAAAG	4m-5	pSeN540	In
pSeW223_F	ATAATAGCTGATGATCCTGATGCTAATGAACCAATTTCAA	4m-5	pSeN540	In
pSeW223_R	ATAAAAGTGGAGCTCCTGGTAAATACCCAGACGAAAGAAA	4m-5	pSeN540	In
pSeW224_F	ATAATAGCTGATGATCCTGATTTTGCTAATGAACCAATTTC	4m-5	pSeN540	In
pSeW224_R	ATAAAAGTGGAGCTCCTGGTTACCCAGACGAAAGAAAA	4m-5	pSeN540	In
pSeW225_F	ATAATAGCTGATGATCCTGAGTATTTTGCTAATGAACCAA	4m-5	pSeN540	In
pSeW225_R	ATAAAAGTGGAGCTCCTGGTCCAGACGAAAGAAAAATGAA	4m-5	pSeN540	In
pSeW226_F	ATAATAGCTGATGATCCTGATGGGTATTTTGCTAATGAAC	4m-5	pSeN540	In
pSeW226_R	ATAAAAGTGGAGCTCCTGGTGACGAAAGAAAAATGAAAG	4m-5	pSeN540	In
pSeW227_F	ATAATAGCTGATGATCCTGAGTCTGGGTATTTTGCTAATG	4m-5	pSeN540	In
pSeW227_R	ATAAAAGTGGAGCTCCTGGTGAAAGAAAAATGAAAGTTTA	4m-5	pSeN540	In
pSeW228_F	ATAATAGCTGATGATCCTGATTCGTCTGGGTATTTTGC	4m-5	pSeN540	In
pSeW228_R	ATAAAAGTGGAGCTCCTGGTAGAAAAATGAAAGTTTATGG	4m-5	pSeN540	In
pSeW229_F	ATAATAGCTGATGATCCTGATCTTTCGTCTGGGTATTTTG	4m-5	pSeN540	In
pSeW229_R	ATAAAAGTGGAGCTCCTGGTAAAATGAAAGTTTATGGACG	4m-5	pSeN540	In
pSeW230_F	ATAATAGCTGATGATCCTGATTTTCTTTCGTCTGGGTATT	4m-5	pSeN540	In
pSeW230_R	ATAAAAGTGGAGCTCCTGGTATGAAAGTTTATGGACGTG	4m-5	pSeN540	In